INSTITUTE OF PHYSICS PUBLISHING EUROPEAN JOURNAL OF PHYSICS

Eur. J. Phys. **26** (2005) 579–587 doi:10.1088/0143-0807/26/4/003

Visualizing the attraction of strange attractors

Matjaž Perc

Department of Physics, Faculty of Education, University of Maribor, Koroška cesta 160, SI-2000 Maribor, Slovenia

E-mail: matjaz.perc@uni-mb.si

Received 6 March 2005
Published 6 May 2005
Online at stacks.iop.org/EJP/26/579

Abstract

We describe a simple new method that provides instructive insights into the dynamics of chaotic time-continuous systems that yield strange attractors as solutions in the phase space. In particular, we show that the norm of the vector field component that is orthogonal to the trajectory is an excellent quantity for visualizing the attraction of strange attractors, thus promoting the understanding of their formation and overall structure. Furthermore, based on the existence of zero orthogonal field strengths in planes that form low-dimensional strange attractors, we also provide an innovative explanation for the origin of chaotic behaviour. For instructive purposes, we first apply the method to a simple limit cycle attractor, and then analyse two paradigmatic mathematical models for classical time-continuous chaos. To facilitate the use of our method in graduate as well as undergraduate courses, we also provide user-friendly programs in which the presented theory is implemented.

M This article features online multimedia enhancements

(Some figures in this article are in colour only in the electronic version)

1. Introduction

More than four decades ago, Lorenz [1] was one of the first to discover that simple nonlinear system equations can display turbulent, inherently unpredictable behaviour, which we now term as chaotic. Since then, interest in the deterministic chaos theory has risen rapidly, and much effort has been invested in integrating it into graduate as well as undergraduate curricula [2–14]. There also exist excellent introductory monographs that explain the basic concepts in a simple and informative manner [15–17].

Deterministic chaos is, despite its rather entangled theoretical background, a very appealing subject. Numerous young people are inspired by the so-called butterfly effect which conveys the message that even small changes in life or the initial conditions of a

dynamical system can have large consequences. Often, however, the initial enthusiasm and motivation for the study are lost when students are unable to comprehend the theory behind chaotic behaviour. This is because widely know facts about chaos are often immediately followed by the introduction of invariant quantities, i.e. quantities that do not depend on initial conditions, such as Lyapunov exponents or entropy and information dimensions [18], which are predominantly used for characterizing chaotic behaviour. Not surprisingly, students find themselves bedazzled by the large dissimilarity between chaos which inspired them and the reality behind it. Thus, it is of great interest to provide insights into the dynamics of chaotic systems with simpler methods.

In this paper, we introduce a simple method that provides instructive insights into the dynamics of chaotic time-continuous systems. In particular, we focus on explaining the formation and overall structure of strange attractors, as well as provide a rather innovative explanation for the extreme sensitivity to changes in initial conditions, which is the hallmark of chaotic behaviour. The method is completely based on the analysis of the system's vector field. Thus, it has a very familiar theoretical background that students acquire very well while studying simple attractors, such as steady states or limit cycles, in the context of the general theory of deterministic dynamical systems. However, since time-continuous dynamical systems have to be at least three dimensional to possibly yield chaotic behaviour, the classical approach of simply plotting the vectors in the phase space often appears muddled, and so does not provide very interesting insights into the dynamics. The virtue of our method lies in the fact that we focus only on those vector field components that are orthogonal to the direction of the trajectory in the phase space, whereby the word 'trajectory' stands explicitly for the attractor of the system and not for trajectories emerging from various initial conditions prior to settling onto the attractor. For phase space points that represent the attractor of the system, the vector field component orthogonal to the trajectory is always the null vector since there the vector field is oriented exactly in the same direction as the trajectory. On the other hand, for phase space points that do not represent the attractor, the vector field component orthogonal to the trajectory is never the null vector since the system is always more or less forced towards the attractor. Thus, by calculating the norm of orthogonal vector field components, we are able to measure just how strong the system is forced towards the attractor in each particular phase space point. To justify our approach and explain the method thoroughly, we first apply it on a simple two-dimensional limit cycle attractor for which vector field components orthogonal to the trajectory can be obtained analytically. Afterwards, we take on the challenge of analysing chaotic systems, for which results must be obtained numerically.

For the studied limit cycle attractor, the method reproduces results that can be inferred also from the standard vector field graph, thus justifying our approach and further applications of the method on chaotic systems. For chaotic systems, the method clearly visualizes forces that shape the strange attractor, and thus provides instructive insights into the dynamics of its formation. Additionally, the method reveals the existence of zero orthogonal field strengths in planes that form strange attractors. Note that low-dimensional chaotic attractors often consist of several planes that are strangely 'melted together' to form the overall fractal geometric structure (see figures 3 and 4). The fact that there exist phase space planes in which there is no force acting towards the reference trajectory can even be viewed as the actual reason why a small deviation from the initial course may result in a large divergence as time progresses, as we will elucidate below. Thereby, our method also provides a rather simple and innovative explanation for the origin of chaotic behaviour in time-continuous systems.

To help the reader reproduce our results, and to facilitate the use of the method in graduate as well as undergraduate courses, we also provide user-friendly programs in which the presented theory is implemented [19].

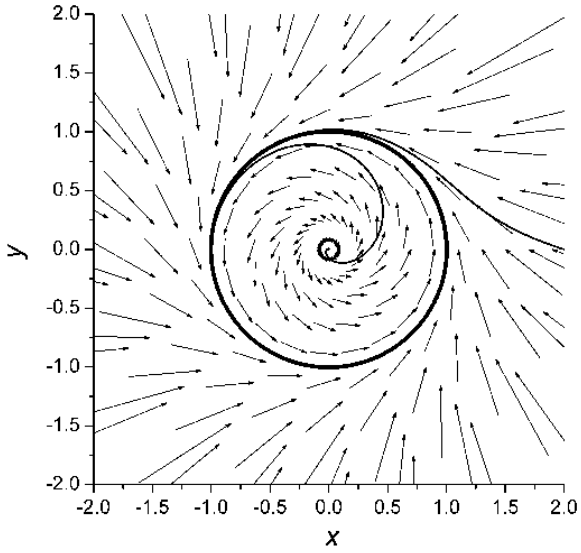

Figure 1. The phase space analysis of the limit cycle attractor. Arrows represent the vector field defined by equations (1) and (2), while the thick solid line represents the limit cycle attractor of the system. Thin solid lines show how the trajectory approaches the attractor from two different initial conditions ($(x_0, y_0) = (0.001, 0.001) \wedge (2.0, 0.0)$). Note how the path of both trajectories is in agreement with the system's vector field.

2. Limit cycle attractor

As outlined in the introduction, to justify our approach and explain the method thoroughly, we first study a simple two-dimensional (2D) limit cycle attractor described with the differential equations:

$$f_x = \mathrm{d}x/\mathrm{d}t = -y + x(1 - x^2 - y^2), \tag{1}$$

$$f_y = \mathrm{d}y/\mathrm{d}t = x + y(1 - x^2 - y^2). \tag{2}$$

The system's vector field $\mathbf{F} = (f_x, f_y)$ and numerical solution are presented in figure 1. It can be observed that, regardless of the initial conditions, equations (1) and (2) yield a circular limit cycle attractor that is centred at the origin of the coordinate system and has unit radius.

Because of the simplicity of the obtained attractor, it is possible to analytically derive the equation for vector field components orthogonal to the trajectory. Again, note that in this context the word 'trajectory' stands explicitly for the attractor of the system and not for trajectories emerging from various initial conditions prior to settling onto the limit cycle. Since the direction orthogonal to the trajectory always equals the radial direction from the origin, it suffices to transform equations (1) and (2) to polar coordinates (r, φ). By substituting $x = r\cos(\varphi)$ and $y = r\sin(\varphi)$ into the above equations, and considering the basic trigonometric relation $\sin^2(\varphi) + \cos^2(\varphi) = 1$, we obtain

$$f_r = \mathrm{d}r/\mathrm{d}t = r(1 - r^2), \tag{3}$$

$$f_\varphi = \mathrm{d}\varphi/\mathrm{d}t = 1, \tag{4}$$

where $f_r\hat{\mathbf{r}}$, $\hat{\mathbf{r}}$ denoting the radial unit vector, is exactly the vector field orthogonal to the limit cycle attractor of the system for all phase space points, whereas variable φ is simply the

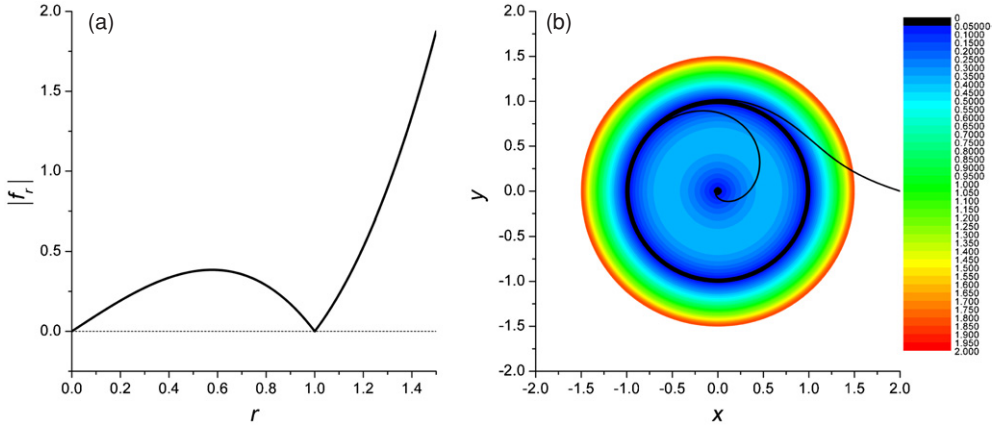

Figure 2. Orthogonal vector field component analysis. (a) The norm of orthogonal vector field components with respect to the limit cycle attractor in polar coordinates. Since in polar coordinates the studied limit cycle attractor transforms to a steady-state value at $r = 1$, a line graph is sufficient to present the results. In general, this is not the case and 2D or 3D colour maps must be used. (b) The norm of orthogonal vector field components with respect to the limit cycle attractor in Cartesian coordinates. Note that the colour map profile from the centre of the coordinate system towards the limit cycle attractor (and beyond) exactly matches the outline of $|f_r|$ presented in (a).

substitute for time. Note that equations (3) and (4) are frequently used in textbooks (e.g. [16]) as an introductory example for systems yielding limit cycle attractors as solutions in the phase space. Here, we have previously introduced Cartesian coordinates to describe our method in a more general setting.

It can be inferred quickly that, in polar coordinates, the system has one unstable fixed point at $r = 0$ and one stable fixed point at $r = 1$, the latter corresponding to the stable limit cycle attractor in Cartesian coordinates. Importantly, note that if $r > 1$ then $f_r < 0$ and if $r < 1$ then $f_r > 0$; either way the system is being forced towards the stable solution at $r = 1$. Since in polar coordinates, the limit cycle attractor corresponds to a stable fixed point, the attraction towards the stable solution of the system can be visualized simply by plotting $|f_r|$ in dependence on r, as shown in figure 2(a), whereby $|f_r|$ directly measures how strong each particular state of the system is forced (0 $\rightarrow$no force, + $\rightarrow$attraction) towards the stable solution. On the other hand, in Cartesian coordinates, a vector field graph depicting $f_r\hat{\mathbf{r}}$, similar to the one presented in figure 1, would be required to convey the same information. However, since we exactly know that each vector $f_r\hat{\mathbf{r}}$ is pointing orthogonal towards the limit cycle attractor, a colour map is better suited for the task. In figure 2(b), colours represent different values of $|f_r|$ that were obtained according to equation (3), whereby the value of the polar coordinate r for various (x, y) was obtained according to $r = \sqrt{x^2 + y^2}$. By comparing figures 1 and 2(b), it can be concluded that they essentially convey the same information. In fact, the above analytical analysis shows that, in the special case of studying a simple 2D point-symmetric limit cycle attractor, our method simply transforms the problem from Cartesian to polar coordinates, i.e. $(x, y) \rightarrow (r, \varphi)$. However, while the classical vector field graph presented in figure 1 also gives precise information about the actual path of the trajectory prior to the system settles onto the attractor, our approach depicted in figure 2(b) yields more concise results, retaining only the information about the attraction in the orthogonal direction with respect to the limit cycle. While for simple 2D systems, our approach boils down to a good exercise clarifying the importance of orthogonal vector field components with respect

to the attractor of the system, its true potential is revealed when applied to three-dimensional (3D) systems that yield strange attractors as solutions in the phase space.

3. Strange attractors

We study two paradigmatic time-continuous systems that yield strange attractors as solutions in the phase space, namely, the Lorenz [1] and the Rössler [20] system. For parameter values $\sigma = 10$, $b = 8/3$ and $r = 25$, the well-known Lorenz system [1] given with the differential equations

$$f_x = \mathrm{d}x/\mathrm{d}t = \sigma(y - x), \tag{5}$$

$$f_y = \mathrm{d}y/\mathrm{d}t = rx - y - xz, \tag{6}$$

$$f_z = \mathrm{d}z/\mathrm{d}t = xy - bz \tag{7}$$

has a chaotic solution, characterized by a strange attractor in the phase space, as presented in figure 3. Note that the attractor is actually made up of planes that melt together continuously towards the bottom, thereby forming the overall geometric structure with the fractal dimension 2.05 [16]. The locally planar structure of the attractor manifests clearly in the fractal dimension that is only slightly above 2, the latter being the exact dimension of a single plane.

The second set of ordinary nonlinear differential equations that we study is represented by the Rössler system [20]:

$$f_x = \mathrm{d}x/\mathrm{d}t = -y - z, \tag{8}$$

$$f_y = \mathrm{d}y/\mathrm{d}t = x + ay, \tag{9}$$

$$f_z = \mathrm{d}z/\mathrm{d}t = c + z(x - g). \tag{10}$$

For parameter values $a = c = 0.2$ and $g = 5.0$, the Rössler system also displays chaotic behaviour on a strange attractor, as presented in figure 4. Again, the locally planar structure of the attractor can be well observed. In the continuation, we study how such intriguing solutions in the phase space (see figures 3 and 4) come into existence, and propose a simple innovative explanation for the extreme sensitivity to changes in initial conditions, which is the hallmark of chaotic behaviour.

To obtain a deeper insight into the formation of low-dimensional strange attractors in the phase space, we apply the method outlined in section 2. However, since the studied chaotic systems cannot be solved analytically, and thus the direction of the trajectory in a particular part of the attractor is neither trivial nor known in advance, we have to resort to numerical calculations. First, we have to approximate the direction of the numerically obtained trajectory at a particular time t. This is done simply by assigning a vector $\mathbf{e}$ to two consecutive points of the trajectory, whereby the first is the one at time $t - \mathrm{d}t$, $\mathrm{d}t$ being the numerical integration step, and the second is the one at time t. Next, we have to determine neighbouring points around the trajectory at time t, in which we want to calculate the norm of orthogonal vector field components, i.e. the analogue to $|f_r|$ introduced in section 2. The most natural way of defining a neighbourhood of points around a line in a 3D phase space, which in our case is the trajectory, is to sample them in concentric circles with variable radius R, whereby the planes defined by the circles should be orthogonal to the direction of the trajectory $\mathbf{e}$, as shown schematically in figure 5. In order to construct the circular planes, we transform the Cartesian coordinates of the trajectory to spherical coordinates, i.e. $(x, y, z) \rightarrow (r, \vartheta, \varphi)$, and then for a given R vary φ and ϑ according to $\varphi \rightarrow \varphi + \mathrm{d}\varphi$ and $\vartheta \rightarrow \vartheta + \mathrm{d}\vartheta$, respectively, whereby

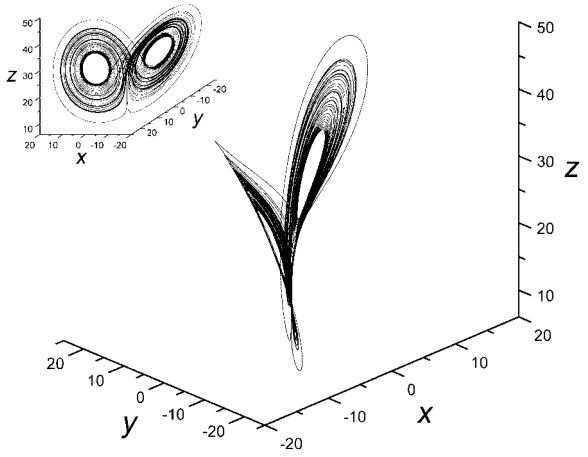

Figure 3. A different view of the Lorenz attractor. It can be well observed that the attractor actually consists of planes that continuously melt together one into another towards the bottom, thereby forming the overall fractal geometric structure. The small insert shows the more traditional view. For parameter values, see the text pertaining to equations (5)–(7).

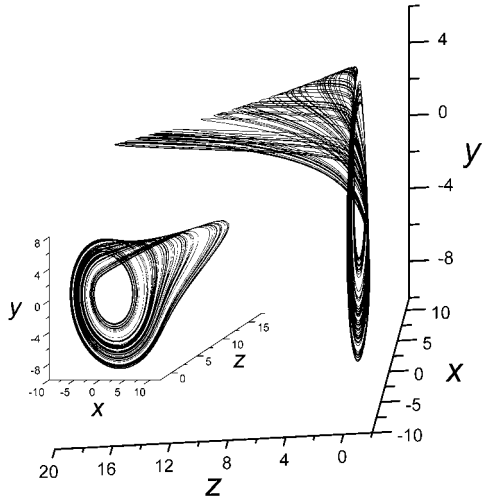

Figure 4. The chaotic Rössler attractor. As in figure 3, it can be well observed that the attractor has a locally planar structure. Particularly in the (x, y) plane, this planar structure can be observed extremely well. Again, the small insert shows the more traditional view. For parameter values, see the text pertaining to equations (8)–(10).

$$\mathrm{d}\varphi = \tan^{-1}\left(\frac{\sqrt{R^2 - (r\tan(\mathrm{d}\vartheta))^2}}{r\sin(\vartheta)}\right), \tag{11}$$

and $\mathrm{d}\vartheta$ varies from $-\tan^{-1}(R/r)$ to $+\tan^{-1}(R/r)$. For each combination of R, $\mathrm{d}\vartheta$ and $\mathrm{d}\varphi$, the transformation of spherical coordinates $(r + R, \vartheta + \mathrm{d}\vartheta, \varphi + \mathrm{d}\varphi)$ back to Cartesian coordinates yields points that form concentric circles with radius R around the trajectory at a particular time t. In these points, the full vector field $\mathbf{F} = (f_x, f_y, f_z)$ is calculated according to the differential equations that govern the time evolution of the system (in our case equations (5)–(7) or (8)–(10)). Finally, the component of the vector field that is orthogonal to the direction of

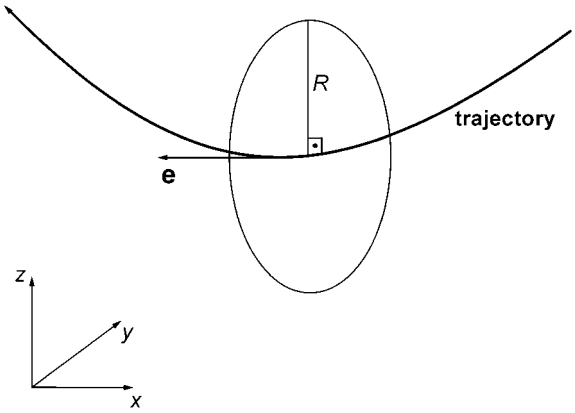

Figure 5. Schematic presentation of the construction of concentric circles with variable radius R around the trajectory in three dimensions. Note that the plane defined by the circle is orthogonal to the direction of the trajectory.

the trajectory $\mathbf{e}$, which we denote as $\mathbf{F}^{\perp} = \left(f_x^{\perp}, f_y^{\perp}, f_z^{\perp}\right)$, is obtained according to the equation [21]

$$\mathbf{F}^{\perp} = \mathbf{F} - \lambda \mathbf{e}, \tag{12}$$

where $\lambda = \mathbf{e} \cdot \mathbf{F}/\mathbf{e} \cdot \mathbf{e}$, which yields $\mathbf{e} \cdot \mathbf{F}^{\perp} = 0$ for all points in the circular planes. To obtain instructive results, this procedure should be repeated for a short continuous segment of the trajectory that lies, preferably, in the 'middle' of one of the attractor's planes. Thereby, we obtain a cylindrical tube that stretches over a particular plane of the attractor, as shown in figure 6. Moreover, since we know the direction of all orthogonal vector field components it is not necessary to plot $\mathbf{F}^{\perp}$ as vectors. Thus, as already argued in section 2, a colour map is the best choice for the task, whereby the colour of each particular point in the circular planes is determined by $\|\mathbf{F}^{\perp}\| = \sqrt{f_x^{\perp^2} + f_y^{\perp^2} + f_z^{\perp^2}}$, which is the direct analogue to $|f_r|$ introduced in section 2. By following the above-described algorithm, we believe that the implementation and graphic presentation of the method should not pose too difficult a task. However, since the method is also intended for undergraduate students, we provide user-friendly programs with graphical interface to facilitate its use and popularity [19].

Finally, we have all at hand to evaluate the results. In figure 6, the method is implemented on the Lorenz (left) and the Rössler (right) system. It can be well observed that, in general, the norm of orthogonal vector field components increases with increasing R, i.e. the distance from the reference trajectory that lies in the middle of the cylindrical tube. However, the increase of orthogonal vector field strengths is much larger in directions that are perpendicular to the plane of the attractor, while in directions on the attractor plane itself the increase is minute. To see this more clearly from several different perspectives, see also the multimedia attachment pertaining to this paper (available online at stacks.iop.org/EJP/26/579). Note that these initial observations apply to both systems, thereby indicating the generality of obtained results and conclusion drawn from it.

Thus, results presented in figure 6 show that each state of the system that lies above or below the plane of the attractor is heavily forced towards the plane, which clearly explains the very formation of planes that form strange attractors. On the other hand, the planes themselves appear to be 'frictionless' in the sense that deviations from the initial course are not hindered by attracting orthogonal forces acting against the divergence. By seeking those points in

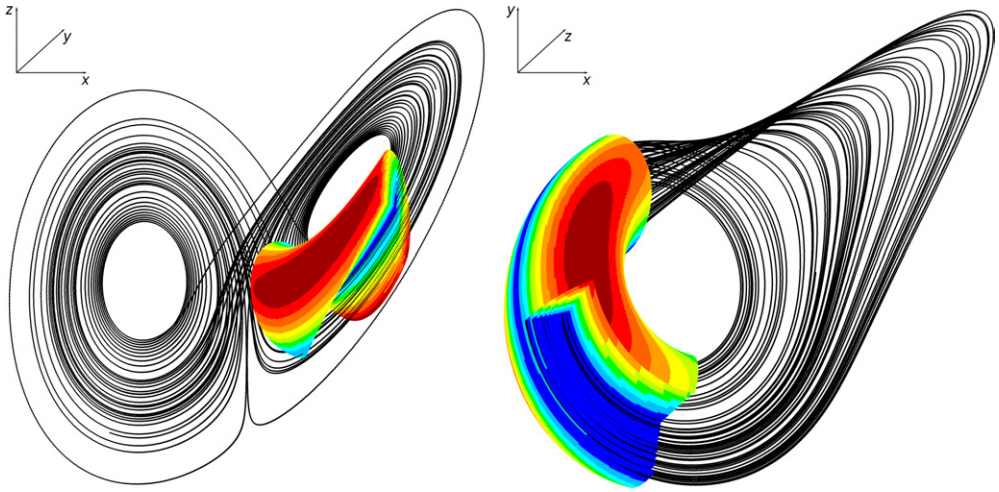

Figure 6. Implementation of the method on the Lorenz (left) and the Rössler (right) system. Colours represent norms of orthogonal vector field components calculated with respect to a short segment of the trajectory that goes through the middle of the cylindrical tube. The vector norm increases in the following colour order: blue, cyan, green, yellow, orange, and red. Thus, the minimal ($\approx$0.0) norm is depicted with blue, while the maximum norm is depicted with red. Note that on both pictures the cylindrical tube has an incision to enable a better view of coloured points that are in the interior. For a view from several different perspectives and the complete colour scale, see the multimedia attachment pertaining to this paper.

the cylindrical tube that are characterized by the minimal orthogonal vector field norm with respect to the reference trajectory, we find that they all lie exactly on the plane of the attractor (see figure 6). Thereby, the dispersion of nearby trajectories in the planes of chaotic attractors can be well explained. In fact, the existence of zero orthogonal field strengths in the planes of chaotic attractors can actually be seen as the very reason why trajectories start to diverge in the first place. A nice analogy can be made with a car driving on an icy road, in our case the road being the plane of the attractor and the car mimicking the trajectory. There, even the slightest change in direction also causes the car to diverge largely from its initial course because there is simply no force that would prevent it from drifting. Thus, the existence of phase space planes in which there is no orthogonal force acting towards the reference trajectory may indeed be viewed as the actual reason why even a small deviation from the initial course may result in a large divergence as time progresses, thereby explaining the origin of chaotic behaviour in time-continuous systems.

4. Summary

In the present paper, we introduce a simple and effective method that provides instructive insights into the dynamics of chaotic time-continuous systems. By visualizing the attraction of strange attractors in the phase space, we are able to explain the formation of planes that form such attractors and give an innovative explanation for the origin of chaotic behaviour. For instructive purposes, we first apply the method on a simple 2D limit cycle attractor, and then analyse two paradigmatic models for time-continuous chaos [1, 20]. In particular, we show that neighbouring trajectories of strange attractors live bounded on planes that are formed by strong orthogonal vector fields acting from above and below, while on the other hand

the planes themselves are, in orthogonal directions with respect to each reference trajectory, 'frictionless' areas due to which small deviations from the original course may grow large as time progresses. Thus, by using the method we can visualize, and more importantly also explain, the formation and overall structure of low-dimensional strange attractors as well as the main characteristic of chaotic behaviour.

Notably, the method is based entirely on the analysis of the system's vector field. Hence, it provides insights into the dynamics of chaotic time-continuous systems by using simple mathematics that students have already acquired during their undergraduate courses while studying the general theory of deterministic dynamical systems. Therefore, we emphasize that the method might be a welcome prelude to existing courses on the theory of deterministic chaos, since it does not interweave with the ergodic theory of chaotic systems. To promote this proposal, we provide user-friendly programs with graphical interface [19], which will hopefully ease the implementation and facilitate the use of our method in graduate as well as undergraduate curricula.

References

[1] Lorenz E N 1963 Deterministic nonperiodic flow *J. Atmos. Sci.* **20** 130–41
[2] MacDonald N and Whitehead R R 1985 Introducing students to nonlinearity: computer experiments with Burgers mappings *Eur. J. Phys.* **6** 143–7
[3] Briggs K 1987 Simple experiments in chaotic dynamics *Am. J. Phys.* **55** 1083–9
[4] Nunez Yepez H N, Salas Brito A L, Vargas C A and Vicente L A 1989 Chaos in a dripping faucet *Eur. J. Phys.* **10** 99–105
[5] Rodgers G J 1992 From order into chaos *Phys. Educ.* **27** 14–7
[6] Carretero-Gonzalez R, Nunez-Yepez H N and Salas-Brito A L 1994 Regular and chaotic behaviour in an extensible pendulum *Eur. J. Phys.* **15** 139–48
[7] Barrientos M, Perez A and Ranada A F 1995 Weak chaos in the asymmetric heavy top *Eur. J. Phys.* **16** 106–12
[8] Borcherds P H 1995 The butterfly that stamped: a brief introduction to nonlinear dynamics and chaos *Phys. Educ.* **30** 372–81
[9] Hobson P R and Lansbury A N 1996 A simple electronic circuit to demonstrate bifurcation and chaos *Phys. Educ.* **31** 39–43
[10] Schmidt T and Marhl M 1997 A simple mathematical model of a dripping tab *Eur. J. Phys.* **18** 377–83
[11] Martin S J and Ford P J 2001 A simple experimental demonstration of chaos in a driven spherical pendulum *Phys. Educ.* **36** 108–14
[12] Gitterman M 2002 Order and chaos: are they contradictory or complementary? *Eur. J. Phys.* **23** 119–22
[13] Tamaševičius A, Mykolaitis G, Pyragas V and Pyragas K 2005 A simple chaotic oscillator for educational purposes *Eur. J. Phys.* **26** 61–3
[14] Kodba S, Perc M and Marhl M 2005 Detecting chaos from a time series *Eur. J. Phys.* **26** 205–15
[15] Schuster H G 1989 *Deterministic Chaos* (Weinheim: VCH)
[16] Strogatz S H 1994 *Nonlinear Dynamics and Chaos* (Reading, MA: Addison-Wesley)
[17] Kaplan D T and Glass L 1995 *Understanding Nonlinear Dynamics* (New York: Springer)
[18] Eckmann J P and Ruelle D 1985 Ergodic theory of strange attractors *Rev. Mod. Phys.* **57** 617–56
[19] http://lizika.pfmb.uni-mb.si/∼matjaz/ejp/chaos.html (All results presented in this paper can be easily reproduced with programs that can be downloaded from this Web page.)
[20] Rössler O E 1976 An equation for continuous chaos *Phys. Lett.* A **57** 397
[21] Bretscher O 1997 *Linear Algebra with Applications* (Englewood, Cliffs, NJ: Prentice Hall)